Lattice density-functional theory of surface melting: the effect of a square-gradient correction

Lattice density-functional theory of surface melting: the effect of a square-gradient correction

Santi Prestipino

Istituto Nazionale per la Fisica della Materia (INFM), UdR Messina, Contrada Papardo,
98166 Messina, Italy
and
Università degli Studi di Messina, Dipartimento di Fisica, Contrada Papardo, 98166 Messina, Italy

Abstract
I use the method of classical density-functional theory in the weighted-density approximation of Tarazona to investigate the phase diagram and the interface structure of a two-dimensional lattice-gas model with three phases—vapour, liquid and triangular solid. While a straightforward mean-field treatment of the interparticle attraction is unable to give a stable liquid phase, the correct phase diagram is obtained when including a suitably chosen square-gradient term in the system grand potential. Taking this theory for granted, I further examine the structure of the solid–vapour interface as the triple point is approached from low temperature. Surprisingly, a novel phase (rather than the liquid) is found to grow at the interface, exhibiting an unusually long modulation along the interface normal. The conventional surface-melting behaviour is recovered only by artificially restricting the symmetries being available to the density field.

1. Introduction

The statistical behaviour of a spatially inhomogeneous classical fluid (as is the case of the interface between two coexisting bulk phases or that of a fluid in a confined geometry) is best analysed within the (classical) density-functional theory (DFT) [1, 2]. Nowadays, the DFT method is widely recognized as being one of the most accurate theoretical tools in statistical mechanics, as also proved by the increasing number of its applications in the scientific literature[1].

Generally speaking, the DFT provides a functional relation between the thermodynamic grand potential of the system and its local-density profile $n(x)$. In practice, the exact relation is not known and one must resort to approximations: typically, good thermodynamic properties of the solid phase are obtained by using only the structural properties of the fluid phase as

---

[1] The *Journal of Physics: Condensed Matter* has recently dedicated a whole issue, the 46th of vol 14 (2002), to the classical DFT method.

input. For instance, in the so-called 'weighted-density approximation' (WDA) [3, 4], one maps the free energy $F[n]$ of the inhomogeneous system onto the free energy of a fluid with a smoothed density $\bar{n}(x)$, which is related in a non-local way to $n(x)$. Another popular DFT is the fundamental-measure theory (FMT) [5] which, by enforcing dimensional crossover, provides the best theory invented so far for the hard-sphere solid [6]. Recently, the FMT has been extended to hard-core lattice gases by Lafuente and Cuesta [7] and soft-repulsive systems by Schmidt [8]. While both the WDA and the FMT work pretty well for purely repulsive systems, they must at present be used in tandem with perturbation theory when the interaction between particles has an attractive component as well [9–13]. In this case, however, there is no guarantee that the DFT answer will be accurate.

Recently, I have carried out (together with Giaquinta) a WDA study [14] of a lattice-gas system with a realistic phase diagram (i.e. one hosting a solid, a liquid and a vapour phase) [15], showing the effectiveness of the DFT method also for lattice problems. However, the theory of [14] uses different prescriptions, in the solid and in the fluid phase, for the contribution of the interparticle attraction to the free energy and this may represent a serious limitation if one is planning to also use the same density functional of the bulk for the interface problem. In particular, an interesting situation to analyse would be that of the solid–vapour interface at a temperature being only slightly below the triple-point temperature. In this case, the melting of the surface usually takes place, with the appearance of a thin liquid layer right at the interface (a successful DFT of this phenomenon for the 3D continuum case can be found in [12]). As a matter of fact, we were not able to provide in [14] sharp evidence of the surface melting since this would rather require that the analytic form of the (approximate) grand potential of the system be unique for all phases.

In the present paper, I develop such a unique density functional for the same lattice model as in [14] by the inclusion of a convenient square-gradient (SG) term. In particular, the new theory leads to a genuine triple point when treating the interparticle attraction as a mean field, thus being a natural candidate for a practical demonstration of the surface-melting phenomenon in a lattice system. The toll of introducing an adjustable parameter into the theory (which, as a result, partly loses contact with the original model) is fully compensated by the gain of a density functional which shares with the exact unknown one a three-minima structure in the triple-point region. It comes as a surprise, however, that this is not sufficient to produce an ordinary surface melting. In fact, an unphysical periodic phase—an artefact of the theory—is unexpectedly found to condense at the solid–vapour interface in place of the liquid. Only by carrying out a suitably constrained minimization of the density functional, aimed at washing out the undesired spurious phase, was I to finally succeed in obtaining the first, at least to my knowledge, DFT description of complete surface melting in a lattice system.

This paper is organized as follows. After a brief outline, in section 2, of the lattice DFT, I describe my system and method in section 3, while presenting results for the bulk and the solid surface in section 4. Finally, a summary of the main conclusions is given in section 5.

2. The lattice density-functional theory: a tutorial

The lattice DFT [16, 17, 14] is a general framework for describing the statistical properties of systems of lattice particles under the influence of a site-dependent external potential ϵ or in the presence of a self-sustained inhomogeneity (e.g. the density modulation of a periodic solid). The statistical description is accomplished in terms of the temperature (T) and chemical-potential (μ) evolution of the local density $n_x = \langle c_x \rangle$, a grand-canonical average of the occupation number $c_x = 0, 1$ of site x in the lattice. n_x is a lattice field which, by the Hohenberg–Kohn–Mermin (HKM) theorem, is in a one-to-one correspondence with the

external field $\mu_x = \mu - \epsilon_x$, allowing one to define the Legendre transform $F[n]$ of the grand potential Ω with respect to the external field. $F[n]$ is the inhomogeneous counterpart of the Helmholtz free energy (a more detailed account of the DFT method can be found in [14]).

Given an external field μ_x, one defines a sort of generalized grand potential:

$$\Omega_\mu[\rho] = F[\rho] - \sum_x \mu_x \rho_x, \tag{1}$$

depending on two lattice fields, ρ and μ, which are regarded as being mutually independent. A minimum principle holds for (1), saying that $\Omega_\mu[\rho]$ attains its minimum for a density profile n_x which is precisely the one determined by μ_x. Moreover, this minimum value is nothing other than the grand potential Ω for the given μ_x. In practice, the exact profile of $F[n]$ is not known (the ideal gas being an outstanding exception) and one should assign a form to $F[n]$ which is then used for deriving, via equation (1), an approximate grand potential for the system.

To help the choice of $F[n]$, one usually works with the derivatives of its excess part $F^{exc}[n] = F[n] - F^{id}[n]$, that is, with the one- and two-point direct correlation functions (DCF) which, in discrete space, are

$$c_x^{(1)}[n] = -\beta \frac{\partial F^{exc}[n]}{\partial n_x} \qquad \text{and} \qquad c_{x,y}^{(2)}[n] = -\beta \frac{\partial^2 F^{exc}[n]}{\partial n_x \, \partial n_y}, \tag{2}$$

where $\beta = 1/(k_B T)$. For a fluid system with density ρ, spatial homogeneity imposes $c_x^{(1)}[n] = c_1(\rho)$ and $c_{x,y}^{(2)}[n] = c_2(x - y, \rho)$. Knowledge of the (two-point) DCF $c_2(x - y, \rho)$ allows one to obtain both the excess free energy $f^{exc}(\rho)$ of the fluid and $c_1(\rho)$ (see [14]).

Once given the fluid properties, the excess free energy of the inhomogeneous system can be formally expressed as an integral of the DCF through

$$\beta F^{exc}[n] = N\rho\beta f^{exc}(\rho) - c_1(\rho) \sum_x (n_x - \rho)$$

$$- \sum_{x,y} (n_x - \rho)(n_y - \rho) \int_0^1 \mathrm{d}\lambda \int_0^\lambda \mathrm{d}\lambda' \, c_{x,y}^{(2)}[n_{\lambda'}], \tag{3}$$

where N is the number of lattice sites and $n_{\lambda x} = \rho + \lambda(n_x - \rho)$. At this point, approximations are no longer eludible since the functional $c_{x,y}^{(2)}[n_{\lambda'}]$ is not known. Among the most popular of these is the WDA [3, 4], which assumes

$$F^{exc}[n] \approx F_{WDA}^{exc}[n] = \sum_x n_x f^{exc}(\bar{n}_x), \tag{4}$$

where the weighted density $\bar{n}_x = \sum_y n_y w(x - y, \bar{n}_x)$. Equation (4) is a refinement of the well-known local-density approximation (LDA), $F_{LDA}^{exc}[n] = \sum_x n_x f^{exc}(n_x)$. In a homogeneous system, $\bar{n}_x$ is required to be constant and equal to the local density, implying a normalization for the weight function w; moreover, w must be such that the fluid DCF also be recovered in the homogeneous limit. This last condition is translated into a well-definite algorithm, which allows one to express $\bar{n}_x$ in terms of the local density. For a lattice system, the details of the WDA method can be found in [14] under the further simplifying hypothesis (first considered by Tarazona [3]) of a weight function being a second-order polynomial in the density.

The final step in the method is the calculation of the difference $\Delta\Omega[n]$ between the generalized grand potential of an inhomogeneous phase (e.g. a crystalline solid) and the fluid one, for equal values of T and μ. One finds

$$\beta\Delta\Omega[n] = \sum_x \left[n_x \ln \frac{n_x}{\rho} + (1 - n_x) \ln \frac{1 - n_x}{1 - \rho} \right] + c_1(\rho) \sum_x (n_x - \rho)$$

$$+ \beta F^{exc}[n] - N\rho\beta f^{exc}(\rho). \tag{5}$$

After minimizing $\Delta\Omega[n]$ over the density field, the phase-coexistence condition is imposed by the vanishing of this minimum difference, which implies the same pressure for both phases.
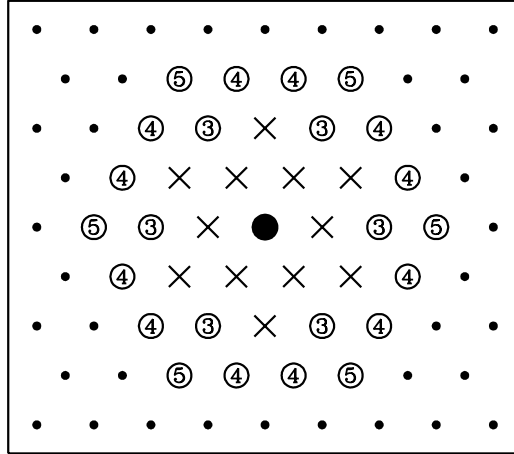
Figure 1. The triangular-lattice model under consideration (schematic): excluded sites ($\times$) and attractive sites (numbered dots) are shown separately for a particle sat at the centre of the picture (large black dot). The attractive interaction reaches the fifth neighbours and no interaction is felt beyond this distance (small dots). The Hamiltonian is of the form $H = \sum_{i<j} v(|i-j|)c_i c_j$, where $v(|i-j|) = +\infty$ when simultaneous occupation of sites i and j is forbidden. In the text, v_n denotes the value of $v(|i-j|)$ for a pair of nth neighbours, whereas z_n is the number of nth neighbours ($z_1 = z_2 = z_3 = 6$, $z_4 = 12$ and $z_5 = 6$). In this work, the interaction strengths were $v_3 = -1.5V$, $v_4 = -1.2V$ and $v_5 = -V$ (with $V > 0$). For these v_n, the phase diagram of the lattice model is the canonical one, with a solid, a liquid and a vapour phase (see [15]).

3. Model and method

As a case study for the surface melting, I shall take a *two-dimensional* (2D) (rather than 3D) lattice-gas model with three phases. By this choice the forthcoming analysis of the interface problem is substantially simplified. Specifically, I consider the t345 model of [15] (see figure 1). This is characterized by a hard-core interaction extending up to second-neighbour sites in the triangular lattice and a pair attraction ranging from third- to fifth-neighbour sites. The interaction strengths are the same as in [14], namely $v_3 = -1.5V$, $v_4 = -1.2V$ and $v_5 = -V$, with $V > 0$. The maximum density allowed for this system is $\rho_{max} = 0.25$. The same model but with $v_3 = v_4 = v_5 = 0$ is called the t model. The role of the t model is that of a reference system since, in the following, the free energy of the inhomogeneous t345 system is going to be estimated through the perturbation-theory formula [1, 14]

$$F[n] = F_0[n] + \sum_{x<y} \Delta v(|x-y|)\langle c_x c_y \rangle_0, \qquad (6)$$

where the subscript 0 refers to the t model and $\Delta v(|x-y|) = v(|x-y|) - v_0(|x-y|)$ is the departure of the t345 pair potential from the reference one (i.e. $\Delta v = 0$ inside the core while $\Delta v = v$ outside). In particular, it is assumed by the mean-field approximation (MFA) that $\langle c_x c_y \rangle_0 = n_x n_y$.

In [14], an approximate DCF for the t fluid is obtained by solving the Ornstein–Zernike relation in the mean-spherical approximation (MSA). It turns out that this MSA solution only exists for all fluid densities ρ up to $\rho = 0.21$. Beyond this threshold, the profile of $f_0^{exc}(\rho)$ is extrapolated as a fourth-order polynomial in the density.

The free energy of the inhomogeneous t system is expressed by the lattice counterpart of the WDA. The further inclusion of the mean-field attraction leads eventually to a density functional for the t345 model which, however, turns out to be insufficient to produce a liquid

basin in the phase diagram [14]. In particular, the value of the freezing density at the critical-point temperature happens to be too small. To overcome this problem, one solution could be to modify the mean-field functional in such a way as to shift the freezing line upward in density, while leaving unaltered the liquid–vapour coexistence locus. To this aim, a simple SG correction is certainly effective: it delays the appearance of the solid phase, thus indirectly promoting the fluid phase. In fact, the SG term has a long tradition, appearing in many popular phenomenological theories of the interface structure [1, 2].

Indeed, a general plausibility argument for the SG correction can be provided, at least in the case of a density field which is slowly varying in space. As discussed in the appendix, the leading terms in the exact perturbative expansion of the excess free energy around a uniform density profile are a LDA free energy plus a SG term. However, finding out a direct link between this term and the microscopic-model parameters is a hard problem (see, however, the appendix). In fact, an even more difficult task could be to present a theoretical justification, within the perturbation theory, for the appearance of a SG correction *near* the mean-field attraction. In particular, including a SG correction into the mean-field functional might lead to overcounting some of the contributions to the free energy. However, if our concern is mainly to formulate a phenomenological DFT theory of surface melting, rather than reproducing a specific model phase diagram, the above objection is only of minor significance. Anyway, an *ad hoc* effective SG correction can always be regarded as just renormalizing the mean-field free energy, i.e. as a means for healing the crudeness of the mean-field attraction by taking into account at least part of the higher-order perturbative corrections. Hence, it makes sense to examine the following form of free energy:

$$\beta F[n] = \sum_x [n_x \ln n_x + (1 - n_x) \ln(1 - n_x)] + \sum_x n_x \beta f_0^{\text{exc}}(\bar{n}_x)$$
$$+ \frac{1}{2} \sum_{x,y} \beta \Delta v(|x - y|) n_x n_y + \frac{1}{2} \sum_x \beta J(n_x) \sum_\delta (n_x - n_{x+\delta})^2, \tag{7}$$

where δ denotes a nearest-neighbour direction and $J(\rho) > 0$ is, at the moment, a still unspecified function of the density and, possibly, also of the temperature. In the spirit of an *entirely* phenomenological approach, the virtue of (7) is to account for the main features of the t345 phase diagram, see section 4.1; then, the same theory will be asked to provide also a sound description of the surface-melting phenomenon.

For the sake of simplicity, a constant value γV is assumed for $J(\rho)$. With this choice, the DFT free energy of the t345 system in units of $k_B T$ becomes equal, in the infinite-temperature, $\beta V \to 0$ limit, to the WDA free energy of the t system in the same units (i.e. the first two terms on the rhs of equation (7)). Moreover, note that the functional of the t model is not influenced by the SG term in equation (7). The value of γ follows after arbitrarily fixing the triple-point density or temperature (see the next section).

In the homogeneous limit, equation (7) gives a generalized grand potential of

$$\frac{\beta \Omega_\mu(\rho)}{N} = \rho \ln \rho + (1 - \rho) \ln(1 - \rho) + \rho \beta f_0^{\text{exc}}(\rho) + \frac{1}{2} \rho^2 \sum_{n=3}^5 z_n \beta v_n - \beta \mu \rho, \tag{8}$$

z_n being the coordination number of the nth lattice shell. The chemical-potential value that makes (8) stationary with respect to ρ is

$$\beta \mu = \ln \frac{\rho}{1 - \rho} - c_{1,0}(\rho) + \rho \sum_{n=3}^5 z_n \beta v_n, \tag{9}$$

where $c_{1,0}(\rho)$ is the one-point DCF of the t model. It has already been discussed in [14] that the functional (8), with $\beta \mu$ as in (9), shows two different minima at low temperature, whence

two fluid phases exist, liquid and vapour, whose relative stability changes upon varying the density ρ.

The solid phase has a triangular crystal structure that can be represented by just two numbers, namely the average densities n_A and n_B at the two sublattices A and B of occupied and unoccupied sites, respectively. The density functional for this phase is then

$$
\frac{4\beta\Omega_\mu(n_A, n_B)}{N} = n_A \ln n_A + (1 - n_A)\ln(1 - n_A) + 3[n_B \ln n_B + (1 - n_B)\ln(1 - n_B)]
$$
$$
+ n_A\beta f_0^{exc}(\bar{n}_A) + 3n_B\beta f_0^{exc}(\bar{n}_B)
$$
$$
+ \frac{1}{2}\left[n_A \sum_{y|x\in A} \beta v(|x - y|)n_y + 3n_B \sum_{y|x\in B} \beta v(|x - y|)n_y \right]
$$
$$
+ \frac{1}{2}\gamma\beta V\left[\sum_{\delta|x\in A}(n_A - n_{x+\delta})^2 + 3\sum_{\delta|x\in B}(n_B - n_{x+\delta})^2 \right] - \beta\mu(n_A + 3n_B). \tag{10}
$$

Upon subtracting (8) from (10) and substituting (9) for $\beta\mu$, one finally arrives, after expanding the sums in (10), at the following expression for $\Delta\Omega$:

$$
\frac{4\beta\Delta\Omega(n_A, n_B)}{N} = n_A \ln \frac{n_A}{\rho} + (1 - n_A)\ln \frac{1 - n_A}{1 - \rho} + 3\left[n_B \ln \frac{n_B}{\rho} + (1 - n_B)\ln \frac{1 - n_B}{1 - \rho} \right]
$$
$$
+ n_A\beta f_0^{exc}(\bar{n}_A) + 3n_B\beta f_0^{exc}(\bar{n}_B) - 4\rho\beta f_0^{exc}(\rho) + 3\beta v_3 n_A^2
$$
$$
+ (12\beta v_4 + 6\beta v_5)n_A n_B + (9\beta v_3 + 12\beta v_4 + 6\beta v_5)n_B^2 - 2\rho^2 \sum_{n=3}^{5} z_n\beta v_n
$$
$$
+ 6\gamma\beta V(n_A - n_B)^2 + \left(c_{1,0}(\rho) - \rho \sum_{n=3}^{5} z_n\beta v_n \right)(n_A + 3n_B - 4\rho). \tag{11}
$$

The weighted densities $\bar{n}_A$ and $\bar{n}_B$ are evaluated from the values of n_A and n_B with the formulae appearing in appendix A of [14]. In practice, the calculation of $\bar{n}_A$ and $\bar{n}_B$ is carried out in parallel with that of n_A and n_B, i.e. by the same iterative procedure which determines the minimum of $\Delta\Omega$. This could be a steepest-descent dynamics or, equivalently, the self-consistent solution of the equations expressing the stationarity condition for $\Delta\Omega$. These equations are easily found to be

$$
n_A^{-1} = 1 + \frac{1 - \rho}{\rho}\exp\left\{ c_1(\rho) - \rho \sum_{n=3}^{5} z_n\beta v_n + \beta f^{exc}(\bar{n}_A) + n_A\beta f^{exc\prime}(\bar{n}_A)\frac{\partial\bar{n}_A}{\partial n_A} \right.
$$
$$
+ 3n_B\beta f^{exc\prime}(\bar{n}_B)\frac{\partial\bar{n}_B}{\partial n_A} + 6\beta v_3 n_A
$$
$$
\left. + (12\beta v_4 + 6\beta v_5)n_B + 12\gamma\beta V(n_A - n_B) \right\};
$$
$$
n_B^{-1} = 1 + \frac{1 - \rho}{\rho}\exp\left\{ c_1(\rho) - \rho \sum_{n=3}^{5} z_n\beta v_n + \beta f^{exc}(\bar{n}_B) + \frac{1}{3}n_A\beta f^{exc\prime}(\bar{n}_A)\frac{\partial\bar{n}_A}{\partial n_B} \right.
$$
$$
+ n_B\beta f^{exc\prime}(\bar{n}_B)\frac{\partial\bar{n}_B}{\partial n_B} + (4\beta v_4 + 2\beta v_5)n_A
$$
$$
\left. + (6\beta v_3 + 8\beta v_4 + 4\beta v_5)n_B + 4\gamma\beta V(n_B - n_A) \right\}.
$$
$$\tag{12}$$

I refer the reader again to [14] for more information about the technicalities of the minimization procedure for $\Delta\Omega$.
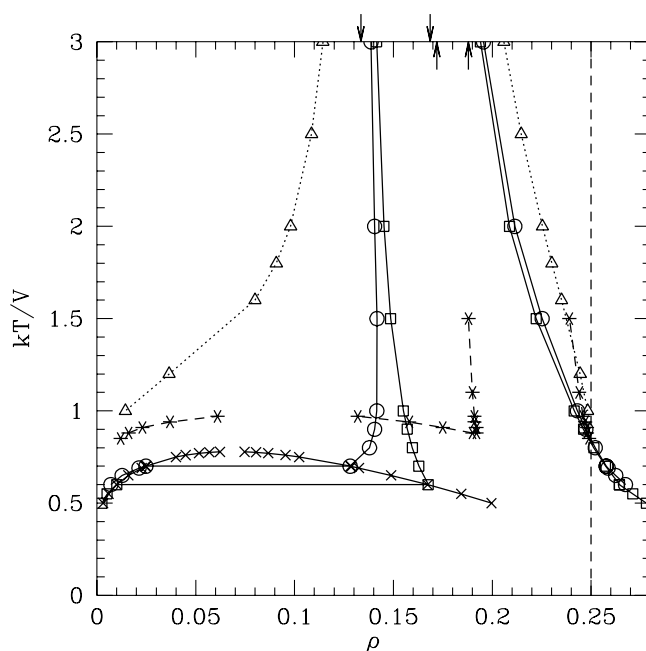
Figure 2. Phase diagram of the t345 model as drawn from the density functional (11), using the t model (MSA + WDA) as a reference and representing the interparticle attraction as a mean-field perturbation. Various solid–fluid coexistence curves are shown: $\gamma = 0$ ($\triangle$ and dotted curves) [14], $\gamma = 0.251\,91$ ($\bigcirc$ and full curves) and $\gamma = 0.282\,14$ ($\square$ and full curves). The liquid–vapour coexistence locus is marked with crosses. For comparison, I have reported (as asterisks joined by broken curves) some MC data points for the 48×48 lattice (the errors affecting these points are of the same size as the symbols). The arrows pointing downwards mark the WDA densities of the coexisting fluid and solid in the t model. The other arrows point to the MC estimates for the same quantities.

4. DFT results

Taken the functional (11) for granted, I now review the results for the bulk properties of the system. Next, I refer to the attempt of using the same functional also for the solid–vapour interface.

4.1. The bulk

First, I summarize the results of the WDA theory for the t model. The coexisting fluid and solid densities are found to be $\rho_f = 0.1335$ and $\rho_s = 0.1686$, respectively [14]. The actual values, obtained through the grand-canonical Monte Carlo (MC) method [14], are instead $\rho_f = 0.172(1)$ and $\rho_s = 0.188(1)$, indicating that the thermodynamic stability of the t solid is overestimated by the theory.

Moving to the attractive model, I first seek the minimum of (8), with $\beta\mu$ as in equation (9). For low enough values of the (reduced) temperature $t = k_B T / V$, there are in fact two distinct points of minimum, the deeper one being associated with the thermodynamically stable phase. The locus of points (ρ, t), where the two minima have equal depth, is the liquid–vapour coexistence line (the crosses in figure 2). In particular, the critical point falls at $\rho_{cr} = 0.068(1)$ and $t_{cr} = 0.778(1)$.
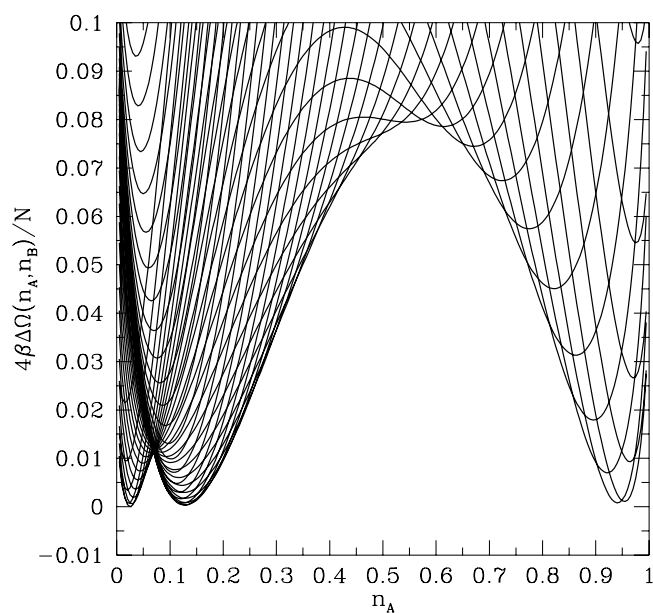
Figure 3. The function $\Delta\Omega(n_A, n_B)$ at equation (11) is plotted versus n_A for various n_B values, ranging from 0 to 1 (both sublattice densities are incremented in steps of 5×10^{-3}). Here, $\gamma = 0.25191$ and $t = t_{tr} = 0.7$. Straight lines are drawn through the points as guides for the eyes. The vapour and liquid densities are $\rho_v = 0.0248$ and $\rho_l = 0.1282$, respectively. The coordinates of the 'solid' minimum are $n_A = 0.94767$ and $n_B = 0.02765$, corresponding to a solid density of $\rho_s = 0.2577$.

As far as the solid–fluid equilibrium is concerned, I first adjust the quantity γ so as to obtain a triple point at a selected temperature t_{tr}. It turns out that, in order for t_{tr} to be, for example, exactly 0.7, the value of γ in (11) has to be 0.25191(1). A slightly larger value, i.e. $\gamma = 0.28214(1)$, shifts the triple-point temperature down to 0.6.

The complete DFT phase diagram of the t345 model is plotted in figure 2 for three values of γ, namely 0 (MFA), 0.25191 ($t_{tr} = 0.7$) and 0.28214 ($t_{tr} = 0.6$). The MC simulation data of [14] are shown as asterisks. It clearly appears that the functional (11) yields a realistic phase diagram only in a small window of γ values. In [14], the predicted DFT phase diagram was equally good (figure 2 of [14], open circles), but we were obliged to use distinct DFT functionals for the solid and the fluid. A minor defect of the present theory is the unphysically large (>0.25) value of the melting density at low temperature. In fact, though n_A and n_B are constrained to be smaller than 1, their combination $n_s = (n_A + 3n_B)/4$ is not under control during the functional minimization. In any event, the agreement of the DFT with MC remains mainly qualitative, also because of the less than excellent quality of the WDA theory for the reference t system.

As already mentioned, the major advantage of (11) over the functional considered in [14] lies in the fact that it has a unique expression for all phases of the system. This is shown, for example, by its profile at the triple-point temperature: for $\gamma = 0.25191$ (i.e. $t_{tr} = 0.7$), the three-minima structure of $\Delta\Omega(n_A, n_B)$ is shown in figure 3, as projected onto the $n_B = 0$ plane in the 3D space spanned by n_A, n_B and $\Delta\Omega$. Upon moving away from the triple point, the relative depth of the minima changes, thus making a particular phase of the system more stable than the others.

4.2. The solid–vapour interface

A density functional with three minima, like that in equation (11), gives the rather unique opportunity to describe on an equal footing, i.e. within the same theoretical framework, both the bulk and the surface statistical properties of a many-particle system. Among these, a prominent place is certainly held by the surface-melting phenomenon, which opens a sort of imaginary window on the structure of the underlying generalized grand potential: roughly speaking, it is the liquid state claiming visibility before thermodynamics gives its allowance.

Let me consider, for instance, a linear interface running along a nearest-neighbour direction, called X. This interface breaks the translational symmetry along the perpendicular, vertical direction Y, thus causing the sublattice densities to have a Y dependence. Very far from the interface, the densities recover the bulk values, being those of the solid for $Y \ll 0$, for example, and those of the coexisting vapour for $Y \gg 0$. The horizontal layers are labelled with an index λ, which increases upon going from solid to vapour, being zero at the 'centre' of the interface. To be specific, those layers where particles are preferentially hosted in the solid have an odd λ value. At variance with the bulk case, *three* sublattices are to be distinguished now, since different density values are generally expected at the even and odd interstitial sites. I call C the sublattice formed by the interstitial sites pertaining to the odd layers and B the other. Finally, A is the triangular sublattice that is occupied in the $T = 0$ solid.

Then, a rather straightforward adaptation of (10) to an interface geometry eventually yields a surplus $\Sigma[n] = 2\beta\Delta\Omega[n]/N_X$ of grand potential per surface particle, due to the interface, equal to

$$
\begin{aligned}
\Sigma[n] = \sum_{\lambda \text{ odd}} & \left[n_{A,\lambda} \ln \frac{n_{A,\lambda}}{\rho} + (1 - n_{A,\lambda}) \ln \frac{1 - n_{A,\lambda}}{1 - \rho} + n_{C,\lambda} \ln \frac{n_{C,\lambda}}{\rho} + (1 - n_{C,\lambda}) \ln \frac{1 - n_{C,\lambda}}{1 - \rho} \right] \\
& + 2 \sum_{\lambda \text{ even}} \left[n_{B,\lambda} \ln \frac{n_{B,\lambda}}{\rho} + (1 - n_{B,\lambda}) \ln \frac{1 - n_{B,\lambda}}{1 - \rho} \right] \\
& + \left(c_{1,0}(\rho) - \rho \sum_{n=3}^{5} z_n \beta v_n \right) \left[\sum_{\lambda \text{ odd}} (n_{A,\lambda} + n_{C,\lambda} - 2\rho) + 2 \sum_{\lambda \text{ even}} (n_{B,\lambda} - \rho) \right] \\
& + \sum_{\lambda \text{ odd}} [n_{A,\lambda} \beta f_0^{\text{exc}}(\bar{n}_{A,\lambda}) + n_{C,\lambda} \beta f_0^{\text{exc}}(\bar{n}_{C,\lambda}) - 2\rho\beta f_0^{\text{exc}}(\rho)] \\
& + 2 \sum_{\lambda \text{ even}} [n_{B,\lambda} \beta f_0^{\text{exc}}(\bar{n}_{B,\lambda}) - \rho\beta f_0^{\text{exc}}(\rho)] + \frac{1}{2} \sum_{\lambda \text{ odd}} \left[n_{A,\lambda} \sum_{y|x\in A,\lambda} n_y \beta \Delta v(|x - y|) \right. \\
& \left. + n_{C,\lambda} \sum_{y|x\in C,\lambda} n_y \beta \Delta v(|x - y|) - 2\rho^2 \sum_{n=3}^{5} z_n \beta v_n \right] \\
& + \sum_{\lambda \text{ even}} \left[n_{B,\lambda} \sum_{y|x\in B,\lambda} n_y \beta \Delta v(|x - y|) - \rho^2 \sum_{n=3}^{5} z_n \beta v_n \right] \\
& + \frac{1}{2}\gamma\beta V \left\{ \sum_{\lambda \text{ odd}} \left[\sum_{\delta|x\in A,\lambda} (n_{A,\lambda} - n_{x+\delta})^2 + \sum_{\delta|x\in C,\lambda} (n_{C,\lambda} - n_{x+\delta})^2 \right] \right. \\
& \left. + 2 \sum_{\lambda \text{ even}} \sum_{\delta|x\in B,\lambda} (n_{B,\lambda} - n_{x+\delta})^2 \right\}.
\end{aligned}
\tag{13}
$$

To save space, some of the sums in the above equation (13) are left as indicated; however, expanding them is not particularly difficult: it is just a matter of carefully looking at the lattice geometry.
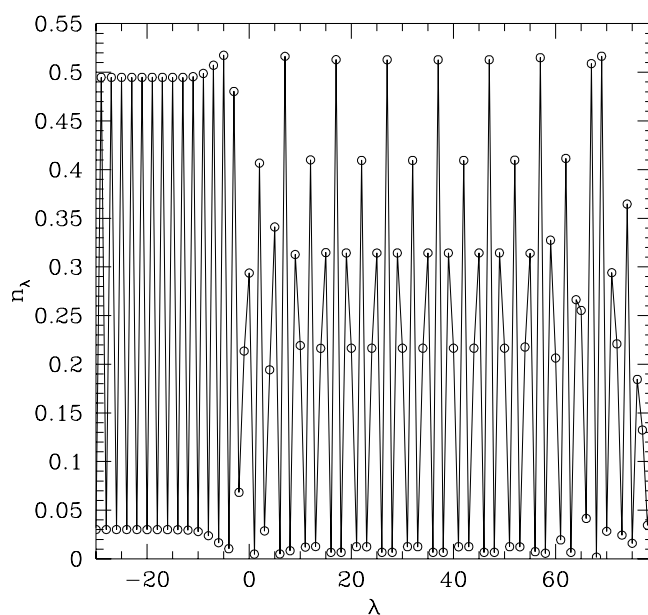
Figure 4. DFT profile of the mean density n_λ at the λth layer, defined as $(n_{A,\lambda} + n_{C,\lambda})/2$ for odd λ and as $n_{B,\lambda}$ for even λ. What is actually plotted is the outcome of the minimization of (13) for $\gamma = 0.251\,91$ and $t = 0.65$. During the minimization process, it is noted that the vapour disappears progressively in favour of a novel phase with a period of ten layers. The automatic search of the minimum $\Delta\Omega$ comes to a stop when this periodic phase reaches the border of the slab.

I have considered the case $\gamma = 0.251\,91$ and a number of temperature values in the range from 0.6 to $t_{tr} = 0.7$. A slab of interface generally consisted of 160 layers, from $\lambda = -80$ to 79, with fixed values of the sublattice densities outside this range. The extension of the slab in the X direction is virtually infinite. The interface is prepared by always assuming an inverted-exponential, $(1 + \exp[(\lambda + 1/2)/l])^{-1}$ modulation [14] which is then relaxed until a minimum of $\Sigma[n]$ is found. Disappointingly, however, the final look of the interface was never as expected. A typical outcome is depicted in figure 4, which refers to $t = 0.65$. We can see that the mean density of a layer, n_λ, shows a curious ten-layer-long periodic motif for $\lambda > 0$, which interrupts at the right border of the picture for the existence of a fixed boundary. Even more serious is the fact that the minimum of $\Sigma[n]$ turns out to be *negative*, signalling that there is something wrong with this interface.

To clarify such things better, I have cut out a piece of this periodic motif and made it infinite in both Y directions. The resulting phase does, in fact, overcome in stability both the solid and the vapour. Obviously, such a weird evidence is totally unphysical, being a spurious result of the DFT, as founded on equation (13). It is worth noticing that, in this periodic phase, the local values of the system density are different at the three sublattices A, B and C, i.e. this phase can only exist in an interface. Nonetheless, the very occurrence of this oddity inevitably casts a shadow on the real quality of the functional (7), which should then be re-examined in spite of its capability of accounting for the bulk properties of the t345 model.

Two different routes are now opening up for our consideration: the first is simply to reject the functional (7) as unphysical. Another solution is, however, viable, which is to insist on (7), trying to see whether it is possible to unveil the normal surface-melting behaviour by properly obstructing the manifestation of the undesired phase. Obviously, this is not completely orthodox since, in a sense, a sort of external field is being introduced into the problem.

If we decide to pursue this second route anyway, one can try the following. Rather than seeking for the absolute minimum of $\Sigma[n]$, the search is restricted to just those fields n_x that, at a particular C site, take the same value as in one of the two closest B sites. Precisely, I require that $n_{C,\lambda} = n_{B,\lambda-1}$, a choice which is consistent with the boundary values but incompatible with the unphysical periodic phase. Whether this is sufficient to promote the appearance of the liquid at the middle of the interface is a matter of debate that can only be fixed numerically.

In order to carry out the constrained minimization of $\Sigma[n]$ along the guidelines presented above, equation (13) must be modified by simply substituting $n_{B,\lambda-1}$ for $n_{C,\lambda}$ everywhere it occurs. A more subtle, but absolutely crucial, technical point is relative to the weighted densities: it follows from their very definition that there is actually no simple relation between $\bar{n}_{C,\lambda}$ and $\bar{n}_{B,\lambda-1}$, even when $n_{C,\lambda} = n_{B,\lambda-1}$. This is due to the fact that, owing to the Y dependence of the sublattice densities, the neighbourhood of a C site does *not* look the same as that of a B site and this causes $\bar{n}_{C,\lambda}$ and $\bar{n}_{B,\lambda-1}$ to be, at least in principle, different. In the end, the amended $\Sigma[n]$ functional is

$$
\begin{aligned}
\Sigma[n] = \sum_{\lambda \text{ odd}} & \left[n_{A,\lambda} \ln \frac{n_{A,\lambda}}{\rho} + (1 - n_{A,\lambda}) \ln \frac{1 - n_{A,\lambda}}{1 - \rho} \right] \\
+ 3 \sum_{\lambda \text{ even}} & \left[n_{B,\lambda} \ln \frac{n_{B,\lambda}}{\rho} + (1 - n_{B,\lambda}) \ln \frac{1 - n_{B,\lambda}}{1 - \rho} \right] \\
+ & \left(c_{1,0}(\rho) - \rho \sum_{n=3}^{5} z_n \beta v_n \right) \left[\sum_{\lambda \text{ odd}} (n_{A,\lambda} - \rho) + 3 \sum_{\lambda \text{ even}} (n_{B,\lambda} - \rho) \right] \\
+ & \sum_{\lambda \text{ odd}} [n_{A,\lambda} \beta f_0^{\text{exc}}(\bar{n}_{A,\lambda}) + n_{B,\lambda-1} \beta f_0^{\text{exc}}(\bar{n}_{C,\lambda}) - 2\rho \beta f_0^{\text{exc}}(\rho)] \\
+ 2 & \sum_{\lambda \text{ even}} [n_{B,\lambda} \beta f_0^{\text{exc}}(\bar{n}_{B,\lambda}) - \rho \beta f_0^{\text{exc}}(\rho)] \\
+ \tfrac{1}{2} & \sum_{\lambda \text{ odd}} \Big\{ n_{A,\lambda}[2\beta v_3(n_{A,\lambda-2} + n_{A,\lambda} + n_{A,\lambda+2}) \\
& + 2\beta v_4(2n_{B,\lambda-3} + n_{B,\lambda-1} + 2n_{B,\lambda+1} + n_{B,\lambda+3}) \\
& + 2\beta v_5(n_{B,\lambda-3} + n_{B,\lambda-1} + n_{B,\lambda+3})] - \rho^2 \sum_{n=3}^{5} z_n \beta v_n \Big\} \\
+ & \sum_{\lambda \text{ even}} \Big\{ n_{B,\lambda}[3\beta v_3(n_{B,\lambda-2} + n_{B,\lambda} + n_{B,\lambda+2}) + \beta v_4(n_{B,\lambda-4} + n_{A,\lambda-3} + 4n_{B,\lambda-2} \\
& + 2n_{A,\lambda-1} + 2n_{B,\lambda} + n_{A,\lambda+1} + 4n_{B,\lambda+2} + 2n_{A,\lambda+3} + n_{B,\lambda+4}) \\
& + \beta v_5(n_{B,\lambda-4} + n_{A,\lambda-3} + n_{B,\lambda-2} + 2n_{B,\lambda} + n_{A,\lambda+1} \\
& + n_{B,\lambda+2} + n_{A,\lambda+3} + n_{B,\lambda+4})] - \tfrac{3}{2}\rho^2 \sum_{n=3}^{5} z_n \beta v_n \Big\} \\
+ \gamma \beta V & \Big\{ \sum_{\lambda \text{ odd}} [3(n_{A,\lambda} - n_{B,\lambda-1})^2 + (n_{A,\lambda} - n_{B,\lambda+1})^2] \\
& + \sum_{\lambda \text{ even}} [(n_{B,\lambda} - n_{A,\lambda-1})^2 + 2(n_{B,\lambda} - n_{B,\lambda-2})^2 + (n_{B,\lambda} - n_{A,\lambda+1})^2] \Big\}. \quad (14)
\end{aligned}
$$

I omit the explicit expression of the weighted densities and their derivatives, since they would need too much space to be specified here.
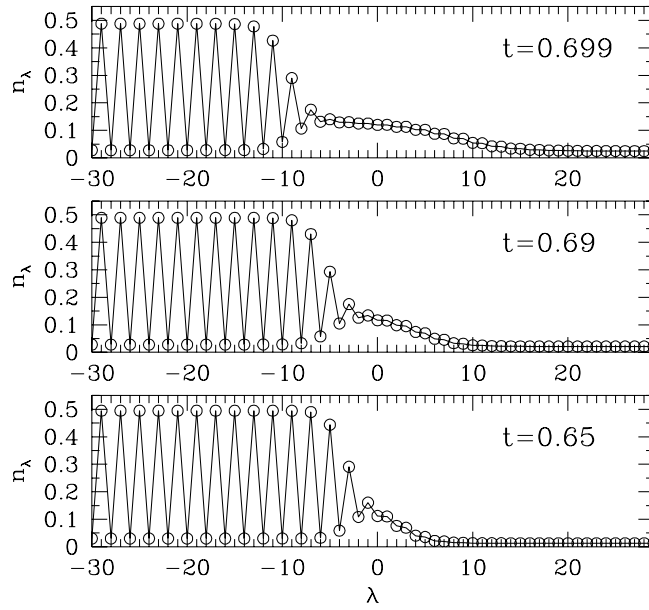
Figure 5. DFT results from the minimization of functional (14) for $\gamma = 0.251\,91$ ($t_{\text{tr}} = 0.7$): the optimum mean-density profile across the solid–vapour interface is plotted for three values of t, namely 0.65, 0.69 and 0.699. To help the eye, in each panel a full line has been drawn through the points. As is quite clear from the pictures, the typical surface-melting behaviour of a 3D simple fluid is derived from equation (14).

Using the functional (14), I have carried out a new series of minimizations for various temperature values. With great pleasure, the thermal evolution of the interface structure is now as expected in a 3D system with a complete surface melting, see figure 5, though dissimilar to the behaviour of the actual (2D) t345 model where the layering of the liquid is much more pronounced, cf figure 9 (top) of [14]. Moreover, the present evidence is also superior to that found in [14] by using different functionals for the fluid and the solid. There, the thickness of the molten layer was too small, even very close to the triple-point temperature.

The slab used in the present optimizations was a hundred layers wide, from $\lambda = -50$ to 49, but only a slice of this is shown in figure 5. In figure 6, I report the detailed profile across the interface of the sublattice densities for two distinct values of t close to t_{tr}, namely $t = 0.69$ and 0.699. By looking at figure 5, we see that the width of the liquid layer grows with regularity as the triple-point temperature is approached from below, corresponding to the liquid phase becoming more and more stable. To estimate this width as a function of temperature, I use the following three-parameter, double-exponential fit:

$$n_{A,\lambda} = \rho + \frac{n_A - \rho_l}{1 + \exp[(\lambda + 1/2 + L)/l_1]} + \frac{\rho_l - \rho}{1 + \exp[(\lambda + 1/2 - L)/l_2]}, \qquad \text{for odd } \lambda \text{ only;}$$

$$n_{B,\lambda} = \rho + \frac{n_B - \rho_l}{1 + \exp[(\lambda + 1/2 + L)/l_1]} + \frac{\rho_l - \rho}{1 + \exp[(\lambda + 1/2 - L)/l_2]}, \qquad \text{for even } \lambda \text{ only;}$$

$$n_{C,\lambda} = n_{B,\lambda-1}, \qquad \text{for odd } \lambda \text{ only.}$$

(15)

In equation (15), ρ_l is the density of the (metastable) liquid coexisting with the vapour at the given temperature $t < t_{\text{tr}}$, $2L$ is the nominal width of the liquified part of the interface, while
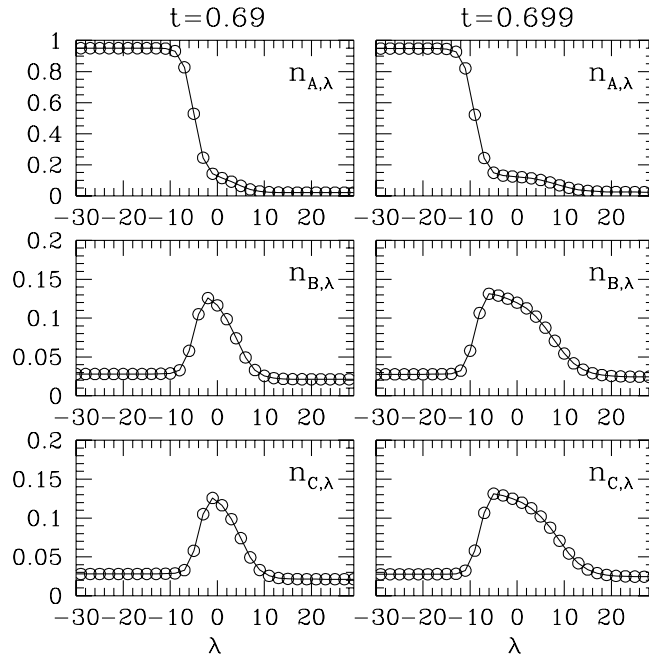
Figure 6. Layer-by-layer evolution of $n_{A,\lambda}$ (for odd λ only), $n_{B,\lambda}$ (for even λ only) and $n_{C,\lambda} = n_{B,\lambda-1}$ (for odd λ only) for the same two interface profiles of highest temperature as in figure 5. Near $\lambda = 0$, the plateau of $n_{A,\lambda}$ and the maximum of both $n_{B,\lambda}$ and $n_{C,\lambda}$ are clear signs of a local liquid-like behaviour.

l_1 and l_2 are a measure of the width of the two transition regions being centred at $-L - 1/2$ and $L - 1/2$, respectively. The values of the fitting parameters are obtained by substituting the ansatz (15) into equation (14) and requiring it to be minimum. It turns out that this minimum value is never appreciably far from the absolute minimum of $\Sigma[n]$ being determined independently.

For $t = 0.65$, 0.69 and 0.699, I find $L = 2.67$, 4.61 and 8.60, respectively (cf figure 5). Hence, while at low temperature it is more convenient for the solid–liquid and liquid–vapour interfaces to stay bound together, slightly below the triple point the free-energy cost of two well-separated interfaces is smaller. In some phenomenological theories of surface melting, this effect is mimicked through the introduction of an effective repulsion between the two interfaces. Furthermore, while $l_1 \simeq 1.0$ shows only a small dependence on temperature, the increase of l_2 with t is more conspicuous, being 1.42, 1.81 and 2.86 for the above cited t values. At these same temperatures, the minimum $\Sigma[n]$ turned out to be 1.101 62, 0.744 72 and 0.655 04, respectively. In particular, the latter value would practically account for the overall cost of two separate solid–liquid and liquid–vapour interfaces at $t = t_{tr}$. I do not try to deduce from the above numbers an empirical relation between $2L$ and t, e.g. with the aim at resolving a logarithmic from a power-law behaviour. In fact, owing to a necessarily imperfect estimate of the coexistence conditions within the DFT, it was actually impossible to approach the triple point more closely than 0.001 in t. This notwithstanding, I do not find any reason to doubt that L would grow to infinity for $t \to t_{tr}^-$.

Summing up, the surface melting is observed, within the functional (11), only at the price of artificially restricting the symmetries that are available to the density field. Otherwise, in fact, a spurious periodic phase will wet the solid, which is actually more stable than the solid and vapour themselves.

5. Conclusions

The usual realm of applications of the classical DFT comprises hard-core systems and soft-repulsive ones. Besides those cases, the only existing general DFT method is, at present, the density-functional perturbation theory which, however, can be quantitatively inaccurate or, even, predict erroneous phase diagrams.

In this paper, I have used the lattice analogue of the perturbative DFT in order to analyse the phase behaviour and the interface structure of a 2D lattice-gas model with a pair interaction consisting of a hard core plus an attractive tail. From previous studies, this model is known to exhibit a solid, a liquid and a vapour phase.

In order to obtain a phase diagram with three phases, I have considered a phenomenological density functional which, besides treating the interparticle attraction as a mean field, also contains a tuneable SG correction. In fact, the very unique request for this theory was to yield a generalized grand potential for an inhomogeneous phase that could exactly turn, in the homogeneous limit, into the fluid functional. This requirement is crucial for getting a consistent description of the interface between the solid and a fluid phase.

After producing a good theory for the bulk, I have adapted the same density functional to the geometry of a solid–vapour interface. The aim was to observe, under equilibrium conditions, the melting of the solid surface, i.e. the growth of a liquid layer between the solid and the vapour as the triple point is approached from low temperature.

Surprisingly, the minimization of the interface functional unveils instead a periodic phase which is totally unphysical, being actually an artefact of the theory. In order to recover a more conventional behaviour, I have carried out a constrained functional minimization which, while not affecting the liquid, makes it unlikely for more exotic phases to appear. By this stratagem, and not withstanding the partial arbitrariness that is implicit in such a conditioned minimization, in the end I arrive at a fairly realistic description of the complete surface melting of a lattice system—a result which, in my opinion, is an interesting illustrative example of the risks which may accompany the use of a phenomenological DFT functional. Anyway, I do not think that the *ad hoc* expedient that was considered here can be of help for investigating, in the absence of a good-quality functional, more delicate features like, for example, layering phase transitions and roughening.

Appendix. Estimate of the square-gradient correction

In this appendix, I show how to adapt to a discrete space an argument originally due to Evans about the estimate of the 'optimal' SG correction to a LDA functional [1].

Let the following excess free energy be considered,

$$F^{\text{exc}}[n] = \sum_x n_x f^{\text{exc}}(n_x) + \tfrac{1}{2} \sum_x J(n_x) \sum_\delta (n_x - n_{x+\delta})^2, \qquad (A.1)$$

which is a LDA free energy supplemented with a SG term. This form of $F^{\text{exc}}[n]$ is not precisely the one which I work with in section 3 for demonstrating the surface-melting phenomenon. Actually, my intention here is not to provide a full justification of equation (7); rather, I just want to give a flavour of the physical status of a SG correction.

To state the problem precisely, the function $J(\rho)$ in equation (7) will be calculated from the requirement that at least the second-order expansion of (A.1) around a fluid of density ρ may agree with the exact one:

$$F^{\text{exc}}[n] = N\rho f^{\text{exc}}(\rho) - \frac{1}{\beta} c_1(\rho) \sum_x \Delta n_x - \frac{1}{2\beta} \sum_{x,y} c_2(x - y, \rho) \Delta n_x \Delta n_y + \cdots. \qquad (A.2)$$

The field $\Delta n_x = n_x - \rho$ is a measure of the (admittedly small) deviation of the system from homogeneity.

Since

$$c_1(\rho) = -\beta f^{\text{exc}}(\rho) - \rho\beta f^{\text{exc}\prime}(\rho), \tag{A.3}$$

the expansion of the LDA term in (A.1) is as follows:

$$\sum_x n_x f^{\text{exc}}(n_x) = N\rho f^{\text{exc}}(\rho) - \frac{1}{\beta}c_1(\rho)\sum_x \Delta n_x - \frac{1}{2\beta}c_1'(\rho)\sum_x \Delta n_x^2 + \cdots. \tag{A.4}$$

To proceed further, it is convenient to work in Fourier space. I take the Fourier transform of a lattice field f_x to be $\tilde{f}_q = \sum_x f_x \exp(-iq \cdot x)$ (see the precise definition of the q vectors in reference [17] of [14]). The convolution theorem first yields

$$\sum_x \Delta n_x^2 = \frac{1}{N}\sum_q \tilde{\Delta n}_q \tilde{\Delta n}_{-q}. \tag{A.5}$$

Similarly, the fully quadratic leading SG correction becomes as follows:

$$\frac{1}{2}J(\rho)\sum_{x,\delta}(n_x - n_{x+\delta})^2 \equiv J(\rho)\sum_{x,y} W(x-y)\Delta n_x \Delta n_y = J(\rho)\frac{1}{N}\sum_q \tilde{W}_q \tilde{\Delta n}_q \tilde{\Delta n}_{-q}. \tag{A.6}$$

The function W in equation (A.6) is lattice-dependent; for example, for a d-dimensional hypercubic lattice with unit lattice constant, $W(x-y) = 2d\delta_{x,y} - \delta_{|x-y|,1}$ and $\tilde{W}_q = 2d[1 - (1/d)\sum_{\alpha=1}^d \cos q_\alpha]$. Finally

$$\sum_{x,y} c_2(x-y, \rho)\Delta n_x \Delta n_y = \frac{1}{N}\sum_q \tilde{c}_2(q, \rho)\tilde{\Delta n}_q \tilde{\Delta n}_{-q}. \tag{A.7}$$

Upon comparing equations (A.4)–(A.6) with (A.7), one would be led to identifying $c_1'(\rho) - 2\beta J(\rho)\tilde{W}_q$ with $\tilde{c}_2(q, \rho)$. However, it is clear that there is no chance for these two quantities to be exactly equal, since $J(\rho)$ does not depend on q. To fix this problem, one should make some further assumptions on the Δn_x. For instance, one can require that, besides being small, Δn_x also varies slowly in space. In this case, only the long-wavelength Fourier components of Δn_x are important, implying that what really matters, in fact, is the matching of the above two quantities in the small-q limit. In particular, the LDA free energy (i.e. $J(\rho) = 0$) does exactly reproduce only the $q = 0$ Fourier component in equation (A.7), since $c_1'(\rho) = \tilde{c}_2(0, \rho)$.

At second order in q

$$\tilde{c}_2(q, \rho) = \sum_x c_2(x, \rho)(1 - iq \cdot x - \tfrac{1}{2}(q \cdot x)^2 + \cdots). \tag{A.8}$$

The first term $\sum_x c_2(x, \rho) = \tilde{c}_2(0, \rho)$. The second term is zero for a lattice with inversion symmetry (i.e. one with $c_2(x, \rho) = c_2(-x, \rho)$). The third term is

$$-\tfrac{1}{2}\sum_x c_2(x, \rho)(q \cdot x)^2 = -\tfrac{1}{2}q^2\sum_x x^2 c_2(x, \rho)(\hat{q} \cdot \hat{x})^2$$

$$= -\frac{1}{2d}q^2\sum_x x^2 c_2(x, \rho) \equiv d_2(\rho)q^2, \tag{A.9}$$

having denoted unit vectors by a hat. Observe that, in the last step, the axial symmetry of the lattice with respect to each coordinate axis has been assumed. Hence, the expansion of $\tilde{c}_2(q, \rho)$ in powers of q begins as $\tilde{c}_2(0, \rho) + d_2(\rho)q^2$.

Since $\tilde{W}_q = q^2 + o(q^2)$ for a hypercubic lattice, the expression of $J(\rho)$ for this lattice is

$$J(\rho) = -\frac{1}{2\beta}d_2(\rho) = \frac{1}{4\beta d}\sum_x x^2 c_2(x, \rho). \tag{A.10}$$

For a triangular lattice, $\tilde{W}_q = (3/2)q^2 + o(q^2)$ while $d_2(\rho)$ is like in equation (A.9) with $d = 2$. Hence, $J(\rho)$ is still given by equation (A.10), but with $d = 3$ (the rationale being that, for the triangular lattice, the nearest-neighbour sites are six, as for the cubic lattice).

To conclude, I make some comments on the result (A.10). For the t model, the non-zero core values of $c_2(x, \rho)$ are all negative, hence $J(\rho) < 0$. This means that the SG correction is meaningless for this model. The case of the t345 model is different, where the positive tail of the DCF would eventually make $J(\rho) > 0$. However, the exact $c_2(x, \rho)$ is not known and this actually makes equation (A.10) rather useless.

References

[1] Evans R 1979 *Adv. Phys.* **28** 143
[2] Recent review articles on the DFT method, with special reference to the freezing of 3D continuous fluids, are
  Baus M 1990 *J. Phys.: Condens. Matter* **2** 2111
  Singh Y 1991 *Phys. Rep.* **207** 351
  Evans R 1992 *Fundamentals of Inhomogeneous Fluids* ed D Henderson (New York: Dekker) p 85
  Löwen H 1994 *Phys. Rep.* **237** 249
[3] Tarazona P 1985 *Phys. Rev.* A **31** 2672
[4] Curtin W A and Ashcroft N W 1985 *Phys. Rev.* A **32** 2909
[5] The literature on the fundamental-measure theory is vast. Here, I list just a few contributions, among the most significant, by its founder: Rosenfeld Y 1989 *Phys. Rev. Lett.* **63** 980
  Rosenfeld Y, Schmidt M, Löwen H and Tarazona P 1997 *Phys. Rev.* E **55** 4245
  Rosenfeld Y 2002 *J. Phys.: Condens. Matter* **14** 9141
[6] Tarazona P and Rosenfeld Y 1997 *Phys. Rev.* E **55** R4873
  Rosenfeld Y and Tarazona P 1998 *Mol. Phys.* **95** 141
  Tarazona P 2000 *Phys. Rev. Lett.* **84** 694
  Tarazona P 2002 *Physica* A **306** 243
[7] Lafuente L and Cuesta J A 2002 *Phys. Rev. Lett.* **89** 145701
  Lafuente L and Cuesta J A 2002 *J. Phys.: Condens. Matter* **14** 12079
  Lafuente L and Cuesta J A 2003 *Preprint* cond-mat/0306221
  Lafuente L and Cuesta J A 2003 *Preprint* cond-mat/0308195
[8] Schmidt M 1999 *Phys. Rev.* E **60** R6291
  Schmidt M 2000 *J. Phys.: Condens. Matter* **11** 10163
  See also Sweatman M B 2002 *J. Phys.: Condens. Matter* **14** 11921
[9] Curtin W A and Ashcroft N W 1986 *Phys. Rev. Lett.* **56** 2775
[10] Tang Z, Scriven L E and Davis H T 1991 *J. Chem. Phys.* **95** 2659
[11] Mederos L, Navascues G, Tarazona P and Chacon E 1993 *Phys. Rev.* E **47** 4284
[12] Ohnesorge R, Löwen H and Wagner H 1991 *Phys. Rev.* A **43** 2870
  Ohnesorge R, Löwen H and Wagner H 1994 *Phys. Rev.* E **50** 4801
[13] Sweatman M B 2001 *Phys. Rev.* E **65** 011102
[14] Prestipino S and Giaquinta P V 2003 *J. Phys.: Condens. Matter* **15** 3931
[15] Prestipino S 2000 *Phys. Rev.* E **62** 2177
[16] Nieswand M, Dieterich W and Majhofer A 1993 *Phys. Rev.* E **47** 718
  Nieswand M, Majhofer A and Dieterich W 1994 *Phys. Rev.* E **48** 2521
[17] Reinel D, Dieterich W and Majhofer A 1994 *Phys. Rev.* E **50** 4744